Nigerian Research Journal of Engineering and Environmental Sciences 11(1) 2026 pp. 16-29
p ISSN: 2635-3342; e ISSN: 2635-3350

Nigerian Research Journal of Engineering and Environmental Sciences
Journal homepage: www.rjees.com

Original Research Article

Adsorption Behavior of Al_2O_3 Nanoparticles in the Treatment of Heavy-Metal-Laden Pharmaceutical Effluents

***[1]Okoye, J.N., [1, 2]Egbosiuba, T.C., [1]Umeuzuegbu, J.C., [3]Mustapha, S., [1]Ezeugo, J.O. and [1]Kamuche, T.**

[1]Department of Chemical Engineering, School of Engineering Technology, Chukwuemeka Odumegwu Ojukwu University, Uli, Anambra State, Nigeria.
[2]Faculty of Chemical and Biochemical Engineering, Missouri University of Science and Technology, Rolla, USA.
[3]Department of Chemistry, School of Physical Sciences, Federal University of Technology, Minna, Nigeria.
*okoyejude32@gmail.com

http://doi.org/10.5281/zenodo.21045262

ARTICLE INFORMATION

Article history:
Received 15 Dec. 2025
Revised 08 Apr. 2026
Accepted 19 Apr. 2026
Available online 30 Jun. 2026

Keywords:
Al_2O_3 nanoparticles
Heavy metals
Pharmaceutical wastewater
Adsorption
Wastewater treatment
Langmuir isotherm
Pseudo-second-order kinetics

ABSTRACT

Heavy metal contamination in pharmaceutical wastewater remains a critical environmental concern due to the toxicity of Ni, Fe, Cr, and Pb. This study evaluates aluminum oxide (Al_2O_3) nanoparticles as an efficient adsorbent for the removal of these heavy metals from pharmaceutical effluents. Al_2O_3 nanoparticles were synthesized via a controlled precipitation method and characterized using X-ray diffraction (XRD), high-resolution scanning electron microscopy (HRSEM), Energy dispersive X-ray (EDX), High-resolution transmission electron microscopy (HRTEM), and Selected area electron diffraction (SAED). The XRD patterns confirmed the formation of highly crystalline α-Al_2O_3, while HRSEM images revealed well-defined spherical particles with porous networks, and EDX spectra verified the presence of aluminum and oxygen, indicating high purity. HRTEM and SAED demonstrated distinct lattice fringes and polycrystalline diffraction rings. BET analysis showed a high surface area and mesoporous structure, enhancing adsorption potential. Batch adsorption experiments assessed the effects of contact time, adsorbent dosage, and temperature on removal efficiency. Results indicated rapid adsorption within the first 30 minutes, reaching equilibrium at approximately 50 minutes. Also, removal efficiency increased with dosage, achieving nearly 100% removal at 0.6–0.7 g. Adsorption improved at higher temperatures, indicating an endothermic process. BET isotherm modeling demonstrated strong adsorption affinity, particularly for Cr. Kinetic analysis showed that metal ion uptake followed a pseudo-second-order model, signifying chemisorption. Thermodynamic parameters ($\Delta G < 0$) confirmed the spontaneity of the process. Overall, Al_2O_3 nanoparticles demonstrate strong potential as a low-cost and environmentally sustainable adsorbent for the treatment of heavy-metal-laden pharmaceutical wastewater.

1. INTRODUCTION

Pharmaceutical industries generate large volumes of wastewater containing a complex mixture of organic and inorganic contaminants, including persistent heavy metals (Anliker et al., 2020; Samal et al., 2022; Wilkinson et al., 2022). These effluents contribute significantly to environmental pollution

and water scarcity challenges, particularly in developing regions (Chowdhary et al., 2020; Baggio et al., 2021). Among these pollutants, nickel (Ni), iron (Fe), chromium (Cr), and lead (Pb) are of particular concern due to their toxicity, persistence, and tendency to bioaccumulate in aquatic systems (Ali et al., 2021; Alagan et al., 2023). Exposure to these metals poses serious health risks, including neurological damage, carcinogenicity, and organ dysfunction (Jaishankar et al., 2014; Alagan et al., 2023). Their continuous discharge into the environment poses serious risks to public health and ecological stability, making effective removal strategies essential, (Pratap et al., 2023).

Conventional treatment methods such as chemical precipitation, ion exchange, coagulation–flocculation, and membrane filtration are widely used but often suffer from limitations including high cost, sludge generation, and reduced efficiency at low contaminant concentrations (Ahmed et al., 2021; Altowayti et al., 2022; Nahiun et al., 2021). Adsorption has emerged as a promising alternative due to its operational simplicity, cost-effectiveness, and high efficiency for removing trace heavy metals (Aktar, 2021; Rathi and Kumar, 2021). The effectiveness of adsorption processes largely depends on the characteristics of the adsorbent, including surface area, pore structure, and functional groups (Al-Ghouti and Da'ana, 2020; Saleh, 2022).

Nanomaterials—particularly metal oxide nanoparticles—have gained increasing attention due to their high surface area, tunable physicochemical properties, and enhanced reactivity (Abid et al., 2022; Saravanan et al., 2022; Pandey et al., 2022). Aluminum oxide (Al_2O_3) nanoparticles are especially attractive as adsorbents because of their thermal stability, low cost, chemical inertness, and strong affinity for metal ions (Ziva et al., 2021; Mohammed et al., 2020). Their surface hydroxyl groups enable adsorption through ion exchange, electrostatic interactions, and surface complexation mechanisms (Kosmulski, 2020; Singh et al., 2021). Additionally, Al_2O_3-based nanomaterials have demonstrated promising performance in removing various heavy metals from aqueous systems (Bonyadi et al., 2023; Sassi et al., 2021; Hassan and Mousa, 2023).

Although numerous studies have explored nanomaterials for wastewater remediation, limited research has focused on the simultaneous removal of multiple heavy metals such as Ni, Fe, Cr, and Pb from pharmaceutical effluents using Al_2O_3 nanoparticles (Khan et al., 2022; Damiri et al., 2022). Pharmaceutical wastewater presents unique treatment challenges due to its complex composition, variable pH, high organic load, and presence of competing ions (Ghazal et al., 2022; Moghaddam et al., 2023). These factors can significantly influence adsorption efficiency and mechanism (Chen et al., 2022; Awang et al., 2023). Therefore, evaluating adsorbents under realistic pharmaceutical wastewater conditions is crucial for developing scalable and effective treatment technologies.

This study aims to synthesize Al_2O_3 nanoparticles and evaluate their efficiency in removing Ni^{2+}, Fe^{2+}/Fe^{3+}, Cr^{6+}, and Pb^{2+} from pharmaceutical wastewater. Comprehensive characterization using XRD, HRSEM, EDX, HRTEM, and SAED was conducted to understand the structural and surface properties influencing adsorption,(Zakharov et al., 2021). Batch adsorption experiments were performed to investigate the effects of pH, adsorbent dosage, contact time, and initial metal concentration (Yadav and Dasgupta, 2022). Furthermore, kinetic, isotherm, and thermodynamic analyses were employed to elucidate the adsorption mechanisms (Chen et al., 2022; Al-Ghouti and Da'ana, 2020). The findings provide valuable insight into the potential of Al_2O_3 nanoparticles as efficient and sustainable adsorbents for heavy metal remediation in pharmaceutical wastewater treatment systems.

2. MATERIALS AND METHODS

2.1. Materials

Aluminium trioxonitrate (V) (Al $(NO_3)_3$) were obtained from BDH Chemicals England at 99% purity. Other chemicals used in this work were acquired from Sigma-Aldrich. The analytical-grade chemicals and reagents were used without additional purification.

2.2. Sample Collection and Pretreatment

Pharmaceutical wastewater samples were collected from Dana pharmaceuticals LTD Minna, Niger State, Nigeria. Samples were obtained from various points within the wastewater treatment system to capture a comprehensive overview of the wastewater characteristics. Upon collection, the samples were transported to the laboratory under refrigerated conditions to prevent any alteration in their chemical composition. Prior to analysis, the samples underwent a pre-treatment process to remove large particulates and debris. This involved the use of filtration and centrifugation techniques to clarify the samples, ensuring that subsequent analytical procedures could be performed accurately and reliably. The pre-treated samples were then stored in appropriate conditions for further analysis.

2.3. Methods

2.3.1. Production of Al_2O_3 nanoparticles

The Al_2O_3 nanoparticles were synthesized using the sol-gel technique. Initially, 10 g of Al $(NO_3)_3$•9H2O were fully dissolved in 150 cm^3 of de-ionized water to achieve a 0.18 M concentration. The solution was stirred at room temperature with a magnetic stirrer, and then 15 cm^3 of ethanol was added dropwise. The temperature of the solution was gradually increased to 80 °C, with the pH maintained between 2 and 3. After stirring for 40 to 45 min to allow for gradual evaporation, a sol-gel solution was formed. The resulting product was dried in an oven at 80 °C for 3 h, then cooled to room temperature, yielding a dry white powder (Mohammed *et al.,* 2020).

2.3.2. Characterization of adsorbent

Analytical methods such as XRD, HRSEM, and HRTEM coupled with EDS, and BET was used to characterize the Al_2O_3 nanoparticles. The synthesized samples were extensively characterized to assess their structure, composition, and surface properties. Powdered X-ray diffraction (XRD) was employed to identify mineral phases and evaluate graphitization, with diffractograms recorded over a 2θ range of 20°–90°. Morphological features were examined using high-resolution scanning electron microscopy (HRSEM). For imaging, 0.05 mg of the sample was mounted on carbon adhesive tape, sputter-coated with Au-Pd, and observed at 5 kV. HRSEM equipped with energy dispersive spectroscopy (EDS) further revealed the elemental composition of the adsorbent. Structural details were analyzed using high-resolution transmission electron microscopy (HRTEM). Here, 10 mg of sample was ultrasonically dispersed in methanol, applied onto a copper grid, dried, and examined. Surface area and pore size distributions were determined via Brunauer–Emmett–Teller (BET) analysis. Samples (0.5 g) were degassed under nitrogen at 90 °C for four hours, weighed to confirm mass loss, and analyzed using liquid nitrogen adsorption

2.3.3. Batch adsorption process

The study evaluated how contact time, adsorbent dosage, and temperature affect the removal of metal ions from wastewater using various adsorbents. To assess contact time, 0.2 g of each adsorbent was mixed with 50 cm^3 of wastewater and agitated at 150 rpm for intervals ranging from 0 to 30 min. After filtration, residual metal concentrations were measured by atomic absorption spectrometry (AAS) to identify the optimum contact time. The influence of adsorbent dosage was examined by varying the amount from 0.3 to 1.0 g while maintaining the optimum contact time, under the same agitation conditions. Additionally, temperature effects were studied by treating wastewater samples with 0.2 g of adsorbent at temperatures between 30 °C and 70 °C in a water bath, again using the optimum contact time. All experiments included filtration through Whatman No. 42 filter paper before AAS analysis. The initial and final concentrations of targeted pollutants were determined. The percentage adsorbed and the adsorption capacity were calculated using Equations 1 and 2.

$$\% \text{ Adsorbed} = \frac{(C_o - C_e)}{C_o} \text{x } 100 \quad (1)$$

$$q_e = \frac{(C_o - C_e)V}{m} \quad (2)$$

where q_e is the adsorption capacity or the amount of equilibrium adsorption in mg/g, C_o is the initial metal concentration in mg/L, C_e is the metal concentration at equilibrium or metal concentration at any time, t in mg/l, V is the volume of the solution, and m is the mass of the adsorbent used.

2.3.5. Adsorption kinetics

The kinetics of adsorption of metal ions from wastewater on the adsorbents were studied by applying the pseudo-first-order and pseudo-second-order models. The linear forms of these equations and their relation plots are as follows:

$$\ln(q_e - q_t) = \ln q_e - k_1 t \quad (3)$$

$$\frac{t}{q_t} = \frac{1}{k_2 q_e^2} + \frac{1}{q_e} t \quad (4)$$

where q_e and q_t are the amount of metal ion adsorbed per unit mass of the adsorbent (mg/g) at equilibrium time and time t, respectively, k_1 is the pseudo-first-order rate constant and k_2 is the pseudo-second-order rate constant.

The Elovich equation describes the adsorption kinetics, assuming a heterogeneous distribution of adsorption energies or activation energies.

$$Q = \frac{1}{\beta}\ln(\alpha\beta) + \ln(\beta t) \quad (5)$$

Where α is the initial adsorption rate (mg/g min), and β is surface coverage constant in equation 5 above, activation energy for chemisorption.

2.3.6. Thermodynamic parameters

The mechanism of adsorption was investigated using thermodynamic parameters such as change in Gibbs free energy (ΔG), enthalpy (ΔH), and entropy (ΔS). Thermodynamic parameters were calculated at various temperatures using the following equationS:

$$K_d = \frac{q_e}{C_e} \quad (6)$$

$$\Delta G = -RT\ln K_d \quad (7)$$

$$\Delta G = \Delta H - T\Delta S \quad (8)$$

In Equation 8 the values of ΔG, ΔH, and ΔS were measured in kJ/mol, kJ/mol, and J/molK respectively. T is the absolute temperature (K), R is the universal gas constant (8.314 J/molK).

3. RESULTS AND DISCUSSION

3.1. Characterization

For aluminum oxide (Al_2O_3), or alumina, XRD peaks appearing at 2θ positions of 39.44°, 44.42°, 56.40°, 64.14°, 74.37°, and 82.12° reflect diffraction from certain planes of its crystal structure Figure 1. The α-Al_2O_3 (corundum phase) is the most stable and thermodynamically favored phase of Al_2O_3. Its XRD peaks align with its standard diffraction pattern. These results are in agreement with the JCPDS card 46-1212, a standard generally accepted for α-Al_2O_3 (Suaebah *et al.*, 2024; Mukhopadhyay *et al.*, 2024). The intensity and sharpness of the peaks indicate that they are highly crystalline in nature.

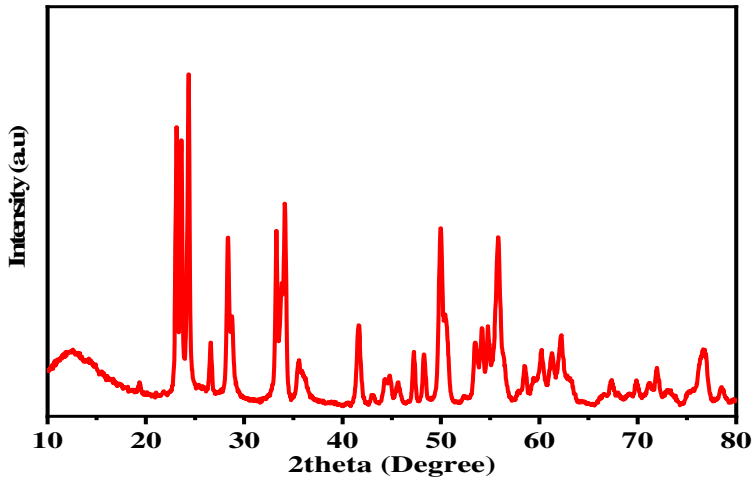

Figure 1: The XRD Patterns of Al_2O_3.

The HRSEM observation of Al_2O_3 gave useful information about the morphological and microstructural features of the material (Figure 2a). The micrographs reveal well-defined grain formations, reflecting the high crystallinity of the alumina formed. The uniform distribution of the grains, as well as the clear grain boundaries, indicates a controlled synthesis process with reduced defects and agglomerates. The HRSEM picture shows that the Al_2O_3 nanoparticles are mostly spherical in nature, with an established network of pores. The interconnecting pores in the alumina matrix enable improved diffusion of the reactants and products (Ren *et al.*, 2024).

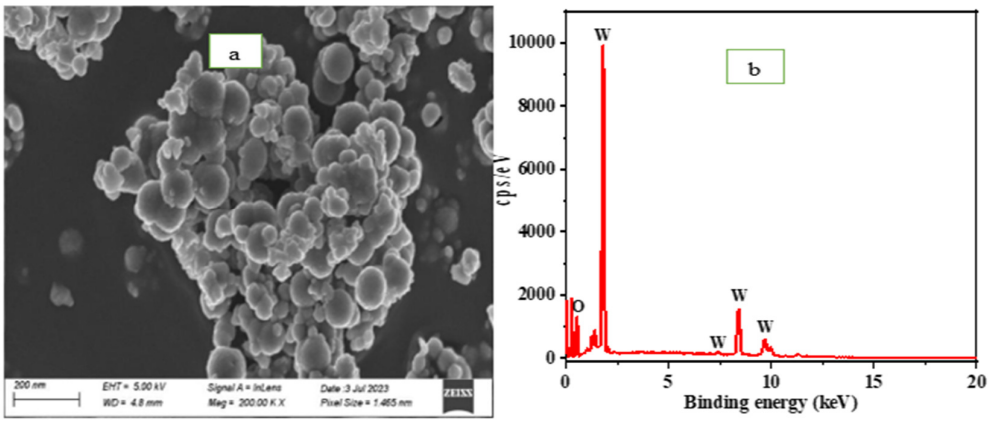

Figure 2: HRSEM image and EDX spectrum of aluminum oxide (Al_2O_3)

The EDX spectrum of Al_2O_3 reveals prominent characteristic peaks for aluminum (Al) and oxygen (O), indicating the presence of the anticipated constituents (Figure 2b). The aluminum peaks are prominent at 1.49 keV (Kα) and 15 keV (Kβ), and oxygen is prominent at around 0.52 keV. For instance, Bokhary *et al.* (2022) reported that EDX of aluminum oxide nanoparticles showed the presence of only aluminum and oxygen, which suggests excellent purity and confirms the stoichiometric constitution of Al_2O_3 as expected. Similarly, Attia *et al.* (2022) determined that the EDX spectrum of Al_2O_3 nanoparticles that were modified presented broad peaks of aluminum and oxygen in notable abundance, again confirming the occurrence of both elements in their expected proportion. Their hardness quantifies stoichiometric Al_2O_3 formation by its proximity to 2:3 ratio between the aluminum atoms to oxygen, representing the strongly established oxide system. Any other peaks lacking indicate high-purity Al_2O_3. The consistent peak distribution of Al and O in different areas of the scan implies uniform composition, while the fluctuations may indicate phase segregation or material inhomogeneity.

The HRTEM image of Al_2O_3 in Figure 3(a) reveals crystalline domains, and the SAED pattern in Figure 3(b) of Al_2O_3 confirms its crystalline nature with diffraction spots indexing to the (110), (113), and (202) planes of the corundum phase. The SAED patterns display rings, which are indicative of a polycrystalline nature. For instance, Ikram et al. (2023) verified that the phase of Al_2O_3 can be verified by diffraction peaks that belong to the (110), (113), and (202) planes, indicating its corundum structure. Similarly, Zhao et al. (2022) stated that the observation of SAED patterns can indicate the polycrystalline nature of materials, in agreement with the findings for Al_2O_3, where the rings in the SAED pattern match numerous orientations of crystallites. In addition, the work of Li et al. (2024) identifies the importance of diffraction peak analysis in determining the microstructural nature of aluminum-based compounds, corroborating the fact that the (110) plane has a distinctive function in determining the crystalline nature of these compounds.

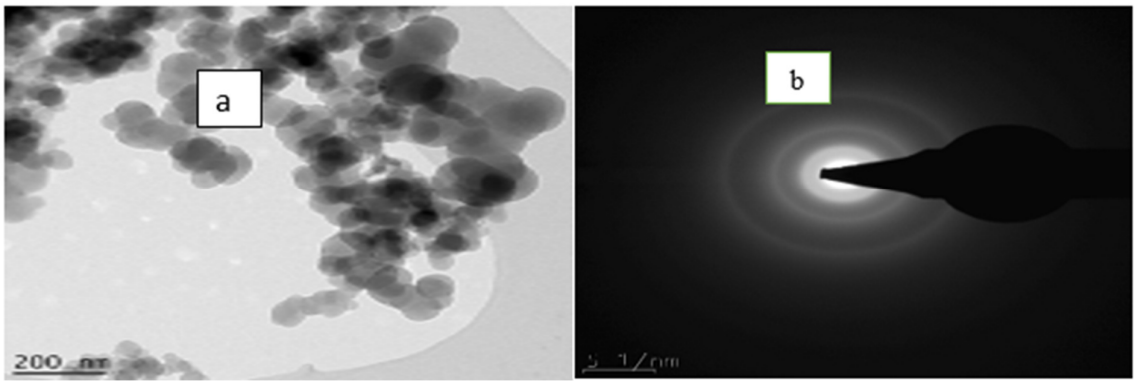

Figure 3: HRTEM and SAED images of Al_2O_3

The plot of adsorption-desorption isotherm curve for Al_2O_3 is shown in Figure 4. The results of BET show that Al_2O_3 has a surface area of 72.38 m^2/g. The large surface area of Al_2O_3 indicates that it may provide a high number of active sites for adsorption. The result also shows that Al_2O_3 possesses a pore size of 8.041 nm. Al_2O_3 having an intermediate pore size, would allow for the adsorption of smaller molecules but still provide sufficient porosity to guarantee efficient mass transfer.

3.2. Removal of Heavy Metals

3.2.1. Contact time

The performance of removal of Cr, Pb, Fe and Ni ions using Al_2O_3 was examined with time (Figure. 5). From the figure, it can be observed that with the increase in contact time, the efficacy of adsorption raises to a peak point. At the initial phase, within 10–30 min, the adsorption rate goes high in all the adsorbents. This quick removal is due to the presence of multiple active binding sites, which allow metal ions to rapidly adsorb onto the adsorbent surfaces (Kaur et al. 2022). Between 30 and 40 min, adsorption continues to increase but at diminishing rates, indicating that active sites are being filled more and more. Competition among metal ions for fewer available binding sites results in a decrease in the rate of adsorption. At 50 min, there is a point of near saturation with little further removal taking place. The trend in the data follows general adsorption principles where there is a fast initial step followed by a slow diminution in the rate of adsorption with increasing saturation of the adsorbent surface (Mayilswamy et al. 2025). The trend follows from previous research work on metal ion removal, where equilibrium is generally attained once binding sites are all occupied.

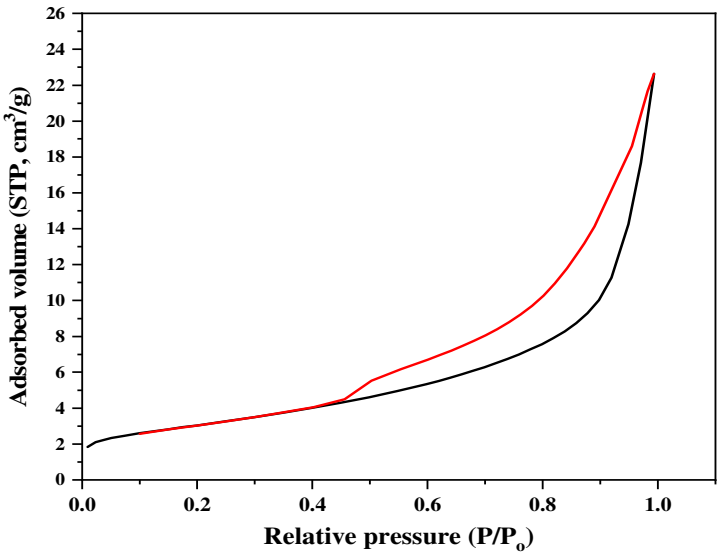

Figure 4: Adsorption-desorption isotherm curves of Al_2O_3

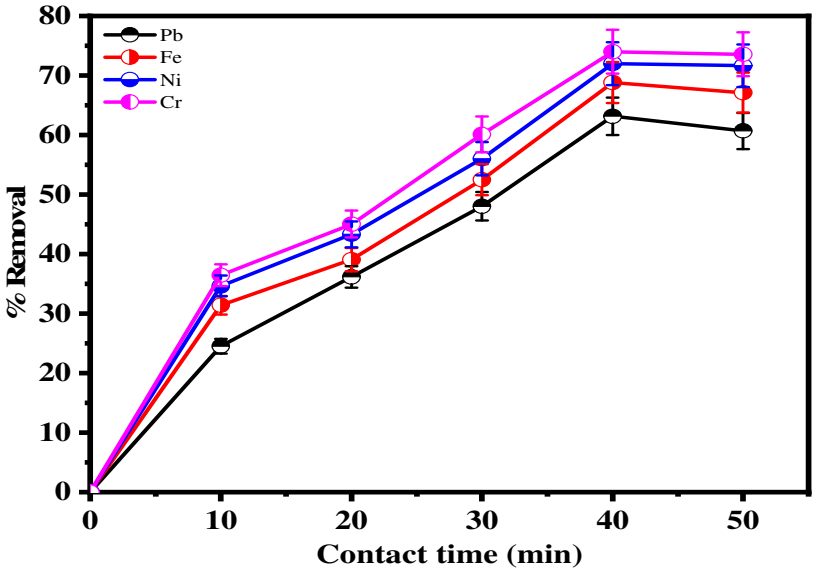

Figure 5: The effect of contact time on the removal of some metal ions using Al_2O_3

3.2.2. Dosage

The removal of Cr, Pb, Fe, and Ni ions at different dosages of adsorbent is depicted in Figure 6. The figure indicates that the dosage of the adsorbent is raised to increase the percentage removal of the metal ions. At a low dose (0.3 g), the removal is extremely low, with Al_2O_3 showing 52.1% removal, removal efficiency increases tremendously due to the enhanced availability of active adsorption sites up to a level where the removal for all the adsorbents at 0.7 g and more is approximately 100%. The observed trend follows the postulation that higher adsorbent doses yield more functional groups and active surface areas for Pb adsorption, thus contributing to improved removal effectiveness (Mahesh et al. 2022). For instance, at 0.5 g, Al_2O_3 removes 79.04% of Pb and at 0.6 g, this observation validates the assumption that while increasing the adsorbent dose increases metal ion removal, there is a threshold

beyond which more adsorbent makes no difference. This saturation is due to an overload in adsorption sites and an overlap of active surface areas, preventing further Pb(II) ions from efficiently interacting with new sites (Hashem et al. 2021). This indicates that there is an optimal dose at the range of approximately 0.6–0.7 g, beyond which maximum removal is obtained, making further increments in dosage redundant.

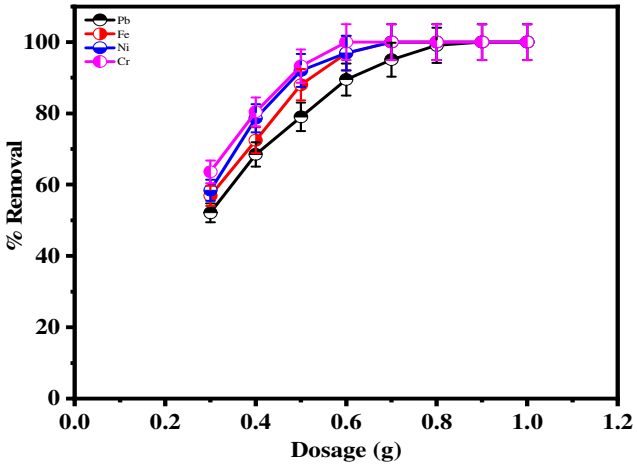

Figure 6: The effect of dosage on the removal of some metal ions using Al_2O_3

3.2.3. Temperature

Figure 7 shows that the adsorption of Cr, Pb, Fe and Ni ions increases with temperature for the adsorbent. This pattern suggests that the process of adsorption is endothermic, i.e., it prefers increasing heat energy. One possible reason for this trend is that increased temperatures give extra kinetic energy to the Pb ions in solution, causing them to travel faster toward the adsorption sites. With increased energy, the ions are able to diffuse more rapidly through the solution and overcome any energy barriers involved in the adsorption process.

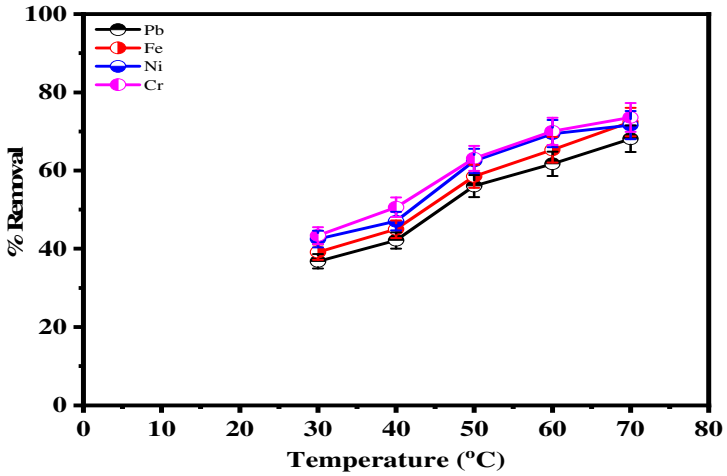

Figure 7: The effect of dosage on the removal of some metal ions using Al_2O_3

As a result, more ions come into contact with and stick to the adsorbent surface. In addition, an increase in temperature can increase the ion exchange capacity of the adsorbent materials (Wu et al. 2021). This phenomenon undergoes structural or surface modifications at elevated temperatures that improve its capacity to adsorb Pb ions. Increased temperature may also affect the surface chemistry of the adsorbents, potentially increasing the density of the active adsorption sites or their affinity towards

heavy metal ions. Increased temperatures may also activate the adsorption sites and the maximum capacity for adsorption at all temperatures, suggesting a synergistic effect among its components. The temperature-dependent increase in Pb adsorption indicates the endothermicity of the reaction. This can be due to increased mobility of ions, improved ion exchange capacity, and activation of adsorption sites, all of which result in enhanced adsorption efficiency at elevated temperatures (Qiu et al. 2021).

3.3. Isotherm Studies

The isotherm parameters in Table 1 offer insights into the adsorption behavior of various metal ions (Ni, Fe, Cr, and Pb) from pharmaceutical wastewater using different models: Freundlich (F), Langmuir (L), Dubinin–Radushkevich (D–R), and Temkin (T). The Freundlich model parameters suggest favorable adsorption, with intensity values (1/n) ranging from 0.496 (Pb) to 0.950 (Cr). All values of $1/n< 1$ indicate favorable multilayer adsorption on heterogeneous surfaces. The correlation coefficients (R^2) for all ions (0.9209–0.9620) confirm the suitability of this model, particularly for Cr. These results align with Mandal et al. (2021) and Li et al. (2022), who reported that the Freundlich model effectively describes adsorption onto Al_2O_3 with heterogeneous surfaces, especially at lower concentrations. The Langmuir constants (q_{max}) range from 76.50 mg/g (Pb) to 105.68 mg/g (Cr), indicating high monolayer adsorption capacity, especially for Cr and Fe. The separation factors (K_L values) between 0.341 (Pb) and 0.945 (Cr) further imply favorable adsorption ($0 < K_L < 1$). Correlation coefficients ($R^2 > 0.91$) suggest a good model fit, particularly for Cr (0.9956) and Fe (0.9936). According to Ramraj et al. (2023) and Vasiraja et al. (2023), a high monolayer capacity and good K_L values reflect strong metal–adsorbent affinity, especially with porous carbonaceous materials. The D–R model's mean free energy (E) values range from 3.920 to 8.163 kJ/mol, indicating that the adsorption mechanism are both physical and chemical (as $E < 9$ kJ/mol). Cr again shows the highest adsorption potential ($E = 8.163$ kJ/mol; $R^2 = 0.9940$), suggesting stronger electrostatic interactions, consistent with findings by Mandal et al. (2021). The model fits all ions well ($R^2 > 0.90$), further validating its application for evaluating energy-based mechanisms. Temkin constants confirm a linear decrease in the heat of adsorption with increasing coverage. Cr and Fe exhibit higher binding energies ($B = 3.742$ and 1.341 J/mol, respectively) and strong correlation coefficients ($R^2 = 0.9915$ and 0.9896), suggesting appreciable adsorbate–adsorbent interactions. These values indicate that metal ion removal is influenced by indirect interactions between adsorbed species, aligning with Li et al. (2022).

Table 1: Isotherm parameters for the removal of some metal ions from pharmaceutical wastewater

Isotherm	Parameter	Ni	Fe	Cr	Pb
F	K_f	0.591	0.602	0.950	0.496
	n	1.310	2.018	1.981	2.770
	R^2	0.9454	0.9519	0.9620	0.9209
L	q_{max}	85.29	98.15	105.68	76.50
	K_L	0.758	0.911	0.945	0.341
	R^2	0.9901	0.9936	0.9956	0.9860
D-R	q_{max}	51.70	65.16	82.42	44.81
	K	2×10^{-7}	2×10^{-8}	2×10^{-9}	1×10^{-6}
	E	5.670	7.715	8.163	3.920
	R^2	0.9880	0.9915	0.9940	0.9715
T	A	0.151	0.780	2.923	0.108
	B	0.959	1.341	3.742	0.786
	R^2	0.9783	0.9896	0.9915	0.9621

3.4. Kinetic Studies

The kinetic data in Table 2 suggest that the adsorption of Ni, Fe, Cr, and Pb ions from pharmaceutical wastewater follows pseudo-second-order kinetics more closely than pseudo-first-order kinetics. This is evidenced by the higher correlation coefficients (R^2) for the pseudo-second-order model (ranging from 0.9915 to 0.9950) compared to the pseudo-first-order model (ranging from 0.8990 to 0.9335S). These findings align with several studies in the literature that indicate chemisorption mechanisms dominate heavy metal adsorption using carbon-based adsorbents. For instance, Melliti et al. (2023) found that the adsorption of metals like Pb and Cr onto date palm fiber-derived activated carbon followed pseudo-second-order kinetics, indicating that the rate-limiting step likely involves valence forces through sharing or exchange of electrons between adsorbent and adsorbate. Similarly, Mubarak et al. (2022) reported that the core–shell nanocomposite of activated carbon/carborundum@microcrystalline cellulose followed pseudo-second-order kinetics for metal adsorption, reinforcing the chemisorption-dominated mechanism. The rate constants (k_2) for the pseudo-second-order model were highest for Cr (6.819 g/mg·min), followed by Fe, Ni, and Pb, indicating that Cr was adsorbed most rapidly. This could be attributed to Cr's higher electronegativity and smaller hydrated ionic radius, which enhances its interaction with active sites on the adsorbent, as similarly noted by Prabu et al. (2022). The Elovich model also provides insights into the adsorption mechanism. Cr and Fe showed relatively higher initial adsorption rates (α) compared to Ni and Pb, indicating a more reactive interaction between these ions and the adsorbent surface. This is consistent with Somyanonthanakun et al. (2023), who found higher Elovich α values for Pb when using nitric acid-modified bagasse-derived carbon, suggesting increased surface heterogeneity and activation due to treatment.

Table 2: Kinetic parameters for the removal of some metal ions from pharmaceutical wastewater

Kinetic	Parameter	Ni	Fe	Cr	Pb
1st	k_1	0.342	0.377	0.414	0.206
	q_e	57.76	76.81	80.50	45.07
	R^2	0.9026	0.9187	0.9335	0.8990
2nd	k_2	4.180	5.109	6.189	3.315
	q_e	81.48	91.13	98.67	72.94
	R^2	0.9915	0.9950	0.9950	0.9918
Elovich	a	0.133	0.718	0.565	0.121
	b	0.119	0.145	0.180	0.094
	R^2	0.9014	0.9240	0.9511	0.8991

3.5. Thermodynamic Studies

The thermodynamic data in Table 3 reveal that the Gibbs free energy change (ΔG) values for the removal of Ni, Fe, Cr, and Pb ions from pharmaceutical wastewater are all negative across the studied temperatures (303–343 K), indicating that the adsorption processes are spontaneous. Furthermore, the magnitude of ΔG becomes more negative as the temperature increases, suggesting that higher temperatures enhance the spontaneity and feasibility of the metal ion removal process. Among the metals, Pb shows the most negative ΔG values, ranging from -38.22 kJ/mol at 303 K to -43.27 kJ/mol at 343 K, indicating the highest affinity of the adsorbent for Pb^{2+}. This trend is followed by Fe (-37.40 to -42.33 kJ/mol), Cr (-37.31 to -42.23 kJ/mol), and Ni (-37.06 to -41.95 kJ/mol). The progressive increase in the magnitude of negative ΔG with temperature across all metals confirms the endothermic nature of the adsorption, aligning with findings from Al-Ma'abreh et al. (2024) and Kongsune et al. (2021), who reported that higher temperatures increase the kinetic energy of metal ions, promoting

better interaction with adsorbent sites. The strong negative ΔG values also suggest chemisorption may be involved, as similarly reported by Nnaji et al. (2021) for Ni adsorption using palm kernel-based activated carbon. Chemisorption typically involves stronger bonds and more negative ΔG values compared to physisorption. This is supported by Al-Hazmi et al. (2024), who highlighted that adsorption mechanisms with ΔG below -20 kJ/mol often indicate chemical interactions. Azam et al. (2022) noted that enhanced metal ion removal at elevated temperatures implies increased randomness at the solid–solution interface, which is consistent with the trend observed here. The increase in temperature likely overcomes activation barriers, facilitating the diffusion of metal ions into internal adsorption sites.

Table 3: Thermodynamic parameters for the removal of some metal ions from pharmaceutical wastewater

Metal	ΔG(kJ/mol)				
	303	313	323	333	343
Ni	-37.06	-38.29	-39.51	-40.73	-41.95
Fe	-37.40	-38.63	-39.86	-41.10	-42.33
Cr	-37.31	-38.54	-39.77	-41.00	-42.23
Pb	-38.22	-39.48	-40.75	-42.01	-43.27

4. CONCLUSION

Al_2O_3 nanoparticles have been successfully tested and demonstrated to be a promising adsorbent for the removal of heavy metals from pharmaceutical wastewater. The Al_2O_3 nanoparticles exhibited a disordered, mesoporous structure with high porosity and oxygen-bearing functional groups, as revealed by XRD, HRSEM, EDX, and HRTEM analyses, which contributed to its adsorption efficiency. The Al_2O_3 nanoparticles shows a higher affinity for Cr, Pb, Fe, and Ni ions, with Cr being most strongly adsorbed across all isotherm models, especially the Langmuir and Freundlich models ($R^2 > 0.98$), due to its higher electronegativity and reactivity. Adsorption performance improves with increasing contact time and temperature, peaking at 50 minutes and demonstrating endothermic behavior driven by enhanced ion mobility and activation of surface sites. A dosage of 0.6–0.7 g of Al_2O_3 nanoparticles achieves nearly 100% removal efficiency for the studied metals, indicating optimal saturation of available sites. Further increases beyond this dosage yield no significant benefits. The adsorption process follows pseudo-second-order kinetics, confirming chemisorption as the dominant mechanism, particularly for Pb and Cr. Negative ΔG values between 303 and 343 K confirm that the process is spontaneous and thermodynamically favorable. Therefore, Al_2O_3 nanoparticles is a sustainable, efficient material for heavy metal sequestration from pharmaceutical effluents.

5. ACKNOWLEDGEMENT

The authors express gratitude to their research supervisors Engr. Dr. T.C. Egbosiuba, Engr. Dr. J.C. Umeuzuegbu for your kind guidance, Engr. Dr. J.O Ezeugo, Dr. Mustapha S., Engr. Kamuche T. , and all their lecturers.

6. CONFLICT OF INTEREST

There is no conflict of interest associated with this work.

REFERENCES

Abid, N., Khan, A.M., Shujait, S., Chaudhary, K., Ikram, M., Imran, M., Haider, J., Khan, M.,Khan, Q. and Maqbool, M. (2022). Synthesis of nanomaterials using various top-down and bottom-up approaches, influencing factors, advantages, and disadvantages: A review. *Advances in Colloid and Interface Science*, *300*, p.102597.

Ahmed, S.F., Mofijur, M., Nuzhat, S., Chowdhury, A.T., Rafa, N., Uddin, M.A., Inayat, A., Mahlia, T.M.I., Ong, H.C., Chia, W.Y. and Show, P.L., 2021. Recent developments in physical, biological, chemical, and hybrid treatment techniques for removing emerging contaminants from wastewater. *Journal of hazardous materials*, *416*, p.125912.

Aktar, J. (2021). Batch adsorption process in water treatment. In *Intelligent Environmental Data Monitoring for Pollution Management* (pp. 1-24). Academic Press.

Alagan, M., Kishore, S.C., Perumal, S., Manoj, D., Raji, A., Kumar, R.S., Almansour, A.I. and Lee, Y.R., 2023. Narrative of hazardous chemicals in water: Its potential removal approach and health effects. *Chemosphere*, 330, p.139178.

Al-Ghouti, M. A., & Da'ana, D. A. (2020). Guidelines for the use and interpretation of adsorption isotherm models: A review. *Journal of hazardous materials*, *393*, p.122383.

Al-Hazmi, H.E., Mohammadi, A., Hejna, A., Majtacz, J., Esmaeili, A., Habibzadeh, S., Saeb, M.R., Badawi, M., Lima, E.C. and Mąkinia, J., 2023. Wastewater treatment for reuse in agriculture: Prospects and challenges. *Environmental Research*, 229, p.116711

Ali, M. M., Hossain, D., Al-Imran, A., Khan, M. S., Begum, M., and Osman, M. H. (2021). Environmental pollution with heavy metals: A public health concern. *Heavy metals-their environmental impacts and mitigation*, (pp.771-783).

Altowayti, W.A.H., Shahir, S., Othman, N., Eisa, T.A.E., Yafooz, W.M., Al-Dhaqm, A., Soon, C.Y., Yahya, I.B., Che Rahim, N.A.N.B., Abaker, M. and Ali, A., 2022. The role of conventional methods and artificial intelligence in the wastewater treatment: a comprehensive review. *Processes*, *10*(9), p.1832.

Al-Ma'abreh,A.M,, AIKhabbas, M, Alawaideh, S, ., Hussein-Al-Ali, S.H., Hmedat, D.A., Edris, G., Abuassaf, R.A. and Hamed, M.A., 2024. Investigation of kinetics, thermodynamics, and isotherms of the simultaneous removal of heavy metal ions by activated carbon from cypress fruit. *Adsorption Science & Technology*, 42, p.02636174241256853.

Anliker, S, Patrick, M, Fenner, K, and Singer, H (2020). Quantification of active ingredient losses from formulating pharmaceutical industries and contribution to wastewater treatment plant emissions. *Environmental Science and Technology*, 54(24), (pp15046-15056).

Attia, K. A., Abdel-Raoof, A. M., Serag, A., Eid, S. M., & Abbas, A. E. (2022). Innovative electrochemical electrode modified with Al 2 O 3 nanoparticle decorated MWCNTs for ultra-trace determination of tamsulosin and solifenacin in human plasma and urine samples and their pharmaceutical dosage form. *RSC advances*, *12*(27), (pp.17536-17549).

Awang, N. A., Wan Salleh, W. N., Aziz, F., Yusof, N., and Ismail, A. F. (2023). A review on preparation, surface enhancement and adsorption mechanism of biochar-supported nano zero-valent iron adsorbent for hazardous heavy metals. *Journal of Chemical Technology & Biotechnology*, *98*(1), (pp.22-44).

Azam, M., Wabaidur, S. M., Khan, M. R., Al-Resayes, S. I., and Islam, M. S. (2022). Heavy metal ions removal from aqueous solutions by treated ajwa date pits: kinetic, isotherm, and thermodynamic approach. Polymers, 14(5), p.914.

Baggio, G., Qadir, M., & Smakhtin, V. (2021). Freshwater availability status across countries for human and ecosystem needs. *Science of The Total Environment*, *792*, p.148230.

Bokhary, K. A., Maqsood, F., Amina, M., Aldarwesh, A., Mofty, H. K., & Al-Yousef, H. M. (2022). Grapefruit extract-mediated fabrication of photosensitive aluminum oxide nanoparticle and their antioxidant and anti-inflammatory potential. *Nanomaterials*, *12*(11), p.1885.

Bonyadi, Z., Fouladi, Z., Robatjazi, A., and Zahmatkesh Anbarani, M. (2023). Reactive red-141 removal from synthetic solutions by γ-Al2O3 nanoparticles: process modeling, kinetic, and isotherm studies. *Applied Water Science*, *13*(2), p.52.

Chen, X., Hossain, M. F., Duan, C., Lu, J., Tsang, Y. F., Islam, M. S., & Zhou, Y. (2022). Isotherm models for adsorption of heavy metals from water-A review. *Chemosphere*, 307, 135545.

Chowdhary, P., Bharagava, R. N., Mishra, S., and Khan, N. (2020). Role of industries in water scarcity and its adverse effects on environment and human health. *Environmental Concerns and Sustainable Development: Volume 1: Air, Water and Energy Resources*, (pp.235-256).

Damiri, F., Andra, S., Kommineni, N., Balu, S.K., Bulusu, R., Boseila, A.A., Akamo, D.O., Ahmad, Z., Khan, F.S., Rahman, M.H. and Berrada, M., 2022. Recent advances in adsorptive nanocomposite membranes for heavy metals ion removal from contaminated water: A comprehensive review. *Materials*, *15*(15), p.5392.

Ghazal, H., Koumaki, E., Hoslett, J., Malamis, S., Katsou, E., Barcelo, D., & Jouhara, H. (2022). Insights into current physical, chemical and hybrid technologies used for the treatment of wastewater contaminated with pharmaceuticals. *Journal of Cleaner Production*, *361*, p.132079.

Hassan, K. H., & Mousa, M. M. (2023, March). Kinetic and thermodynamic studies of Cd (II), Cu (II) and Ni (II) removal in ternary system using ϒ-Al2O3. In *AIP Conference Proceedings. 2475*(1), (pp.020010–020015).

Hashem, A., Aniagor, C. O., Nasr, M. F., & Abou-Okeil, A. (2021). Efficacy of treated sodium alginate and activated carbon fibre for Pb (II) adsorption. International journal of biological macromolecules, 176, (pp.201-216).

Ikram, M., Shahzadi, A., Haider, A., Zain Ul-Abidin, M., Ul-Hamid, A., Yousaf, S.A., Al-Anazy, M.M. and Yousef, E.S., 2023. Outstanding Performance of Mg/g-C3N4-Doped Al2O3 Serving as a Nanocatalyst and Its Bactericidal Behavior: An In Silico Molecular Docking Study. *ACS omega*, *9*(1),(pp.1603-1613).

Kaur, J, Sengupta, P, and Maukhopadhyav, S , (2020). Critical review of bioadsorption on modified cellulose and removal of divalent heavy metals (Cd, Pb, Cu). *Industrial and Engineering Chemistry Research*, 61(5), (pp. 1921-1954).

Khan, A.H., Khan, N.A., Zubair, M., Shaida, M.A., Manzar, M.S., Abutaleb, A., Naushad, M. and Iqbal, J., 2022. Sustainable green nanoadsorbents for remediation of pharmaceuticals from water and wastewater: A critical review. *Environmental Research*, *204*, p.112243.

Kosmulski, M. (2020). The pH dependent surface charging and points of zero charge. VIII. Update. *Advances in Colloid and Interface Science*, *275*, p.102064.

Kongsune, P., Rattanapan, S., and Chanajaree, R. (2021). The removal of Pb2+ from aqueous solution using mangosteen peel activated carbon: Isotherm, kinetic, thermodynamic and binding energy calculation. Groundwater for Sustainable Development, 12, p.100524.

Li, R., Li, Q., Zhang, Z., Zhang, R., Xing, Y., and Han, D. (2024). Effect of Al Content on Microstructure and Properties of AlxCr0. 2NbTiV Refractory High-Entropy Alloys. *Entropy*, *26*(6), p.435.

Li, J., Dong, X., Liu, X., Xu, X., Duan, W., Park, J., Gao, L. and Lu, Y., 2022. Comparative study on the adsorption characteristics of heavy metal ions by activated carbon and selected natural adsorbents. Sustainability, 14(23), p.15579.

Mahesh, N., Balakumar, S., Shyamalagowri, S., Manjunathan, J., Pavithra, M.K.S., Babu, P.S., Kamaraj, M. and Govarthanan, M., 2022. Carbon-based adsorbents as proficient tools for the removal of heavy metals from aqueous solution: a state of art-review emphasizing recent progress and prospects. Environmental research, 213, p.113723.

Mandal, S., Calderon, J., Marpu, S. B., Omary, M. A., & Shi, S. Q. (2021). Mesoporous activated carbon as a green adsorbent for the removal of heavy metals and Congo red: Characterization, adsorption kinetics, and isotherm studies. Journal of Contaminant Hydrology, 243, p.103869.

Mayilswamy, N., Kandasubramanian, B., Nannaware, M., and M. Gore, P. (2025). ANN Modeling for Rhodamine B Adsorption Using Pristine and NaOH-Activated Mesoporous Sewage Sludge Biochars: Kinetic, Isotherm, Thermodynamic, and Regeneration Studies. Industrial & Engineering Chemistry Research.

Melliti, A., Yılmaz, M., Sillanpää, M., Hamrouni, B., & Vurm, R. (2023). Low-cost date palm fiber activated carbon for effective and fast heavy metal adsorption from water: Characterization, equilibrium, and kinetics studies. *Colloids and Surfaces A: Physicochemical and Engineering Aspects*, *672*, p.131775.

Moghaddam, A., Khayatan, D., Esmaeili Fard Barzegar, P., Ranjbar, R., Yazdanian, M., Tahmasebi, E., Alam, M., Abbasi, K., Esmaeili Gouvarchin Ghaleh, H. and Tebyaniyan, H., 2023. Biodegradation of pharmaceutical compounds in industrial wastewater using biological treatment: A comprehensive overview. *International Journal of Environmental Science and Technology*, *20*(5), (pp.5659-5696).

Mohammed, A. A., Khodair, Z. T., and Khadom, A. A. (2020). Preparation and investigation of the structural properties of α-Al_2O_3 nanoparticles using the sol-gel method. *Chemical Data Collections*, *29*, p.100531.

Mubarak, M. F , Zayed, A. M , and Ahmed, H. A (2022). Acivated Carbon/Carborundum@Microcrystalline Cellulose core shell nano-composite: Synthesis, characterization and application for heavy metals adsorption from aqueous solution. Industrial Crops and Products, 182, p.114896.

Mukhopadhyay, A., Pal, A., Sarkar, S., & Megaridis, C. M. (2024). Laser-Tuned Surface Wettability Modification and Incorporation of Aluminum Nitride (AlN) Ceramics in Thermal Management Devices. *Advanced Functional Materials*, *34*(18), p.2313141.

Nahiun, K. M., Sarker, B., Keya, K. N., Mahir, F. I., Shahida, S., & Khan, R. A. (2021). A review on the methods of industrial waste water treatment. *Scientific Review*, *7*(3), (pp.20-31).

Nnaji, C, C ,Agim, A. E , Mama, C. N., Emenike, P. C., & Ogarekpe, N. M. (2021). Equilibrium and thermodynamic investigation of biosorption of nickel from water by activated carbon made from palm kernel chaff. Scientific Reports, 11(1), p.7808.

Pandey, P, Khan, F, Agarwal, S., and Singh, M. (2022). Nano adsorbents in wastewater treatment: a new paradigm in wastewater management. *Lett. Appl. Nanobiosci*, *12*, p.125.

Pratap, B., Kumar, S., Nand, S., Azad, I., Bharagava, R. N., Ferreira, L. F. R., and Dutta, V. (2023). Wastewater generation and treatment by various eco-friendly technologies: Possible health hazards and further reuse for environmental safety. *Chemosphere*, *313*, p.137547.

Prabu, D , Kumar, P. S , Rathi, B.S., Sathish, S., Anand, K.V., Kumar, J.A., Mohammed, O.B. and Silambarasan, P., 2022. Feasibility of magnetic nano adsorbent impregnated with activated carbon from animal bone waste: Application for the chromium (VI) removal. Environmental Research, 203, p.111813.

Qiu, B., Tao, X., Wang, H., Li, W., Ding, X., & Chu, H. (2021). Biochar as a low-cost adsorbent for aqueous heavy metal removal: A review. Journal of Analytical and Applied Pyrolysis, 155,p. 105081.

Ramraj, S. M , Kubaib, A., Imran, P. M., & Thirupathy, M. K. (2023). Utilizing Sida Acuta leaves for low-cost adsorption of chromium (VI) heavy metal with activated charcoal. Journal of Hazardous Materials Advances, 11, p.100338.

Rathi, B. S., and Kumar, P. S. (2021). Application of adsorption process for effective removal of emerging contaminants from water and wastewater. *Environmental Pollution*, *280*, p.116995.

Ren, B., Liu, Y., Yu, J., Wang, T., Jiang, H., Dong, C., Xiong, C., Wang, N., Huang, X. and Hao, H., 2024. Enhancement of high-alumina glass and glass-ceramics through dual modification of Zn 2+ and its mechanism. *Journal of Materials Chemistry A*, *12*(43), (pp.29763-29775).

Saleh, T. A. (2022). Adsorption technology and surface science. In *Interface Science and Technology* (Vol. 34, pp. 39-64). Elsevier.

Samal, K., Mahapatra, S., and Ali, M. H. (2022). Pharmaceutical wastewater as Emerging Contaminants (EC): Treatment technologies, impact on environment and human health. *Energy Nexus*, *6*, p.100076.

Saravanan, A., Kumar, P. S., Hemavathy, R. V., Jeevanantham, S., Jawahar, M. J., Neshaanthini, J. P., & Saravanan, R. (2022). A review on synthesis methods and recent applications of nanomaterial in wastewater treatment: Challenges and future perspectives. *Chemosphere*, p.135713.

Sassi, W., Boubaker, H., Ben-Khaled, H., Dhaoui, S., Ghorbal, A., & Hihn, J. Y. (2021). Modelization and implementation of free adsorption and electrosorption of Cr (VI) from wastewater using Al 2 O 3 nanoparticles: assessment and comparison of the two processes. *Environmental Science and Pollution Research*, *28*, (pp.28349-28366).

Singh, S., Kapoor, D., Khasnabis, S., Singh, J., & Ramamurthy, P. C. (2021). Mechanism and kinetics of adsorption and removal of heavy metals from wastewater using nanomaterials. *Environmental Chemistry Letters*, *19*(3), (pp.2351-2381).

Suaebah, E., Yunata, E. E., & Wijaya, A. S. N. (2024, November). The sintering temperature effect of Alumina (Al2O3) ceramic using the sol-gel method. In *Journal of Physics: Conference Series* (Vol. 2900, No. 1, p. 012044). IOP Publishing.

Somyanonthanakun, W., Ahmed, R., Krongtong, V., and Thongmee, S. (2023). Studies on the adsorption of Pb (II) from aqueous solutions using sugarcane bagasse-based modified activated carbon with nitric acid: kinetic, isotherm and desorption. Chemical Physics Impact, 6, p100181.

Vasiraja, N, Saravana Sathiya Prabhahar, R, Joshua, A (2023). Preparation and Physio–Chemical characterization of activated carbon derived from prosopis juliflora stem for the removal of methylene blue dye and heavy metal containing textile industry effluent, Vol. 397, p.136579.

Wilkinson, J.L , Boxall, A.B., Kolpin, D.W., Leung, K.M., Lai, R.W., Galbán-Malagón, C., Adell, A.D., Mondon, J., Metian, M., Marchant, R.A. and Bouzas-Monroy, A., 2022. Pharmaceutical pollution of the world's rivers. *Proceedings of the National Academy of Sciences*, *119*(8), p. e2113947119.

Wu, J., Wang, T., Wang, J., Zhang, Y., & Pan, W. P. (2021). A novel modified method for the efficient removal of Pb and Cd from wastewater by biochar: Enhanced the ion exchange and precipitation capacity. Science of the Total Environment, 754, p.142150.

Yadav, B. S, and Dasgupta, S. (2022). Effect of time, pH, and temperature on kinetics for adsorption of methyl orange dye into the modified nitrate intercalated MgAl LDH adsorbent. Inorganic Chemistry Communications, 137, p.109203.

Zakharov, N.S , PopovaYadav, A. N , Zakharov, Y. A , Pugachev, V. M., & Russakov, D. M. (2021). Transmission electron microscopy for evaluating the structural parameters of nanoparticles. In *Journal of Physics: Conference Series* (Vol. 1749, No. 1, p. 012011). IOP Publishing.

Zhao, Z., Zou, X., Zhao, Y., Shi, J., Huang, Y., and Wang, J. (2023). Magnetic ion-imprinted microspheres for the removal of heavy metal ions from aqueous solution. *Environmental Progress & Sustainable Energy*, *42*(2), p.e13985.

Ziva, A. Z., Suryana, Y. K., Kurniadianti, Y. S., Nandiyanto, A. B. D., & Kurniawan, T. (2021). Recent progress on the production of aluminum oxide (Al2O3) nanoparticles: A review. *Mechanical Engineering for Society and Industry*, *1*(2), (pp.54-77).